

THE VOID PHENOMENON

P. J. E. PEEBLES

Joseph Henry Laboratories, Princeton University, Princeton, NJ 08544

ABSTRACT

Advances in theoretical ideas on how galaxies formed have not been strongly influenced by the advances in observations of what might be in the voids between the concentrations of ordinary optically selected galaxies. The theory and observations are maturing, and the search for a reconciliation offers a promising opportunity to improve our understanding of cosmic evolution. I comment on the development of this situation and present an update of a nearest neighbor measure of the void phenomenon that may be of use in evaluating theories of galaxy formation.

Subject headings: cosmology: theory — galaxies: formation

1. INTRODUCTION

Voids between the regions occupied by normal textbook galaxies contain few observable galaxies of stars or gas clouds, and, apart from a tendency to greater gas content and star formation rates, objects observed in and near voids seem to be close to a fair sample of the cosmic mix. This striking effect will be termed the void phenomenon. A numerical definition, based on nearest neighbor statistics, is summarized in §3.4.

The void phenomenon may be related to the preferences of early-type galaxies for high density regions and of galaxies rich in gas and star formation for the edges of voids. This morphology-density correlation follows in a natural way from the biased galaxy formation picture in the Gaussian adiabatic cold dark matter (CDM) model. Perhaps the biased formation extends to the voids, where the morphological mix swings to favor dark galaxies. But if this were so the shift to the void mix would have to be close to discontinuous (§2.2), in remarkable contrast to the observed relatively slow variation of morphological mix with ambient density in regions occupied by visible galaxies. From continuity one might have thought the more likely picture is that gravity has emptied the voids of mass as well as galaxies. This does not happen in the CDM model, however. Simulations show, between the concentrations of large dark mass halos, clumps of mass that seem to be capable of developing into void objects observable as clumps of stars or gas, contrary to what is observed.

The apparent discrepancy has not attracted much attention since the introduction of the biased galaxy formation picture fifteen years ago. This is partly because we do not have an established theory of how mass concentrations become observable (though we do have some guidance from the observations of galaxies at ambient conditions that do not seem to be very different from the voids; §4.1). A contributing factor is that the theoretical community has not settled on a standard numerical measure of the void phenomenon. A nearest neighbor statistic is commonly used in the observational community. This is discussed in §3, and §3.4 summarizes an update of the nearest neighbor statistic that might be applied to realizations of galaxy formation models.

The main points of this paper are summarized in §5.1.

Section 5.2 offers comments on the history of the void phenomenon as an example of the complex and occasionally weak interaction of theory and practice in a developing subject like cosmology. The discussion of the observational situation in §2 and §3 and of the theoretical situation in §4 illustrates the unusually lengthy duration of modest interaction between theoretical and observational ideas about voids, and the resulting opportunity now to learn something new.

2. VOIDS AND VOID OBJECTS

2.1. *Voids*

Rood (1981) gives an excellent picture of the state of observational studies of galaxy clustering two decades ago. He remarks that 20 years earlier Mayall (1960, fig. 3) had found that in the direction of the Coma cluster far more galaxies are in the cluster than the foreground. Redshift surveys to larger angular distances from the cluster (Tift & Gregory 1976; Chincarini & Rood 1976; Gregory & Thompson 1978) show Mayall had observed foreground voids¹ with radii² $\gtrsim 20h^{-1}$ Mpc. Jõeveer, Einasto, & Tago (1978) independently identified voids — holes in their terminology — in the galaxy distribution in the southern galactic hemisphere.

Other surveys of galaxy types — dwarf, low luminosity, irregular, low surface brightness, star-forming, or IRAS — that are found to respect common voids include Thompson (1983), Thuan, Gott & Schneider (1987), Eder et al. (1989), Binggeli, Tarenghi & Sandage (1990), Bothun et al. (1993), Linder et al. (1996), Kuhn, Hopp & Elsässer (1997), Schombert, Pildis & Eder (1997), Popescu, Hopp & Elsässer (1997), Lee et al. (2000), and El-Ad & Piran (2000).

The preference of star-forming galaxies for the edges of voids certainly agrees with the biased galaxy formation picture, as Salzer has consistently noted (Salzer, Hanson, & Gavazzi 1990; Lee et al. 2000; and references therein). Salzer also emphasizes the similar large-scale structures. Figure 3 in Lee et al. (2000) clearly illustrates voids de-

¹The statement in Peebles (1993) that Kirshner et al. (1981) named these regions voids is wrong; Kirshner et al. clearly state the prior discussions.

²Hubble's constant is $H_o = 100h$ km s⁻¹ Mpc⁻¹.

fined by both ordinary and emission-line galaxies.

Gas clouds also avoid voids. This applies to gas detected in HI 21-cm emission (Weinberg et al. 1991; Hoffman, Lu & Salpeter 1992; Szomoru et al. 1996; Zwaan et al. 1997) and gas detected at somewhat lower surface densities as Lyman-limit or MgII quasar absorption line systems: when the redshift allows the test a galaxy generally is observed close to the line of sight and near the redshift of each absorption line system (Bergeron & Boisse 1991; Steidel, Dickinson & Persson 1994; Lanzetta et al. 1995). Shull, Stocke & Penton (1996) show that gas clouds detected as very low surface density Lyman α absorbers, with HI surface density $\sim 10^{13} \text{ cm}^{-2}$, avoid dense galaxy concentrations. A visual impression is that they also avoid the voids, but that awaits a numerical test, perhaps along the lines of the nearest neighbor distribution (§3).

2.2. Void Boundaries

The strong clustering of galaxies on small scales must open low density regions. In a clustering hierarchy model that fits the two- through four-point correlation functions of optically selected galaxies (Soneira & Peebles 1978) the void sizes are comparable to what is observed (Soneira 1978; Vettolani et al. 1985). The discovery from redshift maps is that the void boundaries tend to be rather smooth, and defined by galaxies with a broad range of luminosities (Chincarini, Rood & Thompson 1981; de Lapparent, Geller & Huchra 1986).

2.3. Void Objects

Another aspect of the void phenomenon is that isolated galaxies do not seem to be particularly unusual, apart from the gas content. Thus Szomoru et al. (1996) conclude that “the void galaxies [in Boötes] seem to be unaware of the fact that they exist in a huge underdense region.” In an important advance Grogin & Geller (2000) find evidence that the relative velocities of void galaxy pairs at projected separation $< 115h^{-1} \text{ kpc}$ tend to be lower than the relative velocities at near cosmic ambient density. Pairs of galaxies at separation $\sim 100h^{-1} \text{ kpc}$ typically have other neighbors whose massive halos add to the relative velocity, however, so the implication for the correlation of halo mass with ambient density will require further discussion.

2.4. Voids and the Morphology-Density Correlation

The mix of morphological types correlates with ambient density (Hubble 1936; Dressler 1980; Postman & Geller 1984). The new aspect of the void phenomenon is that if there is a special class of void galaxies the shift to the void mix when the ambient density falls below some fraction of the cosmic mean has to be close to discontinuous.

This point seems to have been first made by Kirshner et al. (1981), who note that if the voids were missing galaxies but not mass one might expect low luminosity galaxies are more common relative to $L \sim L_*$ galaxies in voids. But they conclude that if this were so the void galaxies would have to be several magnitudes fainter than typical optically selected galaxies, because these hypothetical faint galaxies are not observed. This agrees with the CfA (Center for Astrophysics) galaxy maps in Figures 2a and 2d of Davis et al. (1982): the distributions of the high and low luminosity galaxies are strikingly similar. The same effect is seen in

the extension of the CfA survey (de Lapparent, Geller & Huchra 1986).

The morphology-density correlation includes the preference of star-forming galaxies for the edges of voids (Thompson 1983; Salzer 1989). But Figure 3 in Grogin & Geller (2000) shows how subtle is the variation of the mix of observed types with ambient density when the density is comparable to the cosmic mean. It can be compared to the very different mix within voids, if there is a dark void population.

2.5. The Most Extraordinary Objects

Extremely unusual galaxies are worth special consideration. The statistics of their environments are insecure, by definition, but the discovery of a few cases well inside voids would be influential. Two examples of quite unusual objects — that happen not to be in voids — may illustrate the situation.

A systematic program of study of the remarkable blue compact galaxy SBS 0335-052 (Thuan & Izotov 1997; Vanzi et al. 2000; Pustil’nik et al. 2000; and references therein) shows it has an extended HI cloud with quite low heavy element abundances along the lines of sight to star-forming regions, quite young star populations, and a large mass-to-light ratio. It has many of the properties one might look for in a young galaxy at low redshift, except its position. The projected distance to the large spiral galaxy NGC 1376 is 150 kpc, at close to the same redshift (Pustil’nik et al. 2000). Figure 1 shows the position of SBS 0335-052 relative to the galaxies in the Optical Redshift Survey (Santiago et al. 1995)³ with heliocentric redshifts in the range $4043 \pm 300 \text{ km s}^{-1}$ centered on SBS 0335-052. This unusual object is not in a dense re-

³ <http://www.astro.princeton.edu/~strauss/ors/index.html>

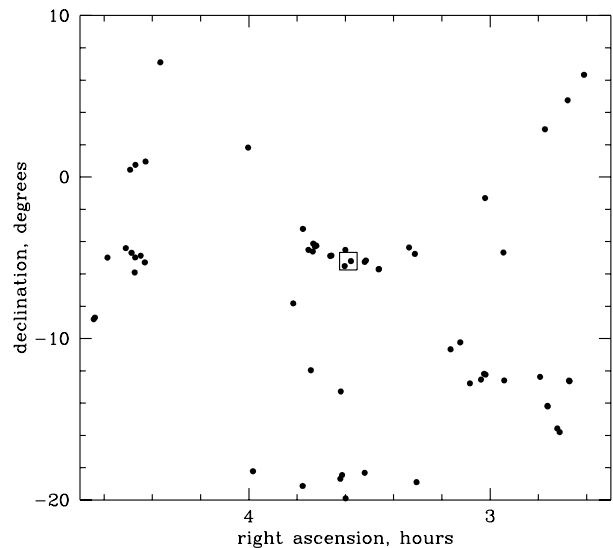


FIG. 1.— Map of Optical Redshift Survey galaxies (filled circles) in a slice in redshift space 600 km s^{-1} deep centered on SBS 0335-052 (open box). The field is $23.5h^{-1} \text{ Mpc}$ wide by $21.3h^{-1} \text{ Mpc}$ high.

gion. More important of the present purpose, it is not in a void. The former agrees with the familiar behavior of star-forming galaxies. The latter does not naturally agree with the biased galaxy formation picture.

A second example is DDO 154. The large ratio of dark to luminous mass led Carignan & Freeman (1988) to term it a “dark” galaxy. It is not far from the Local Group, at supergalactic coordinates $SGL=90^\circ$, $SGB=+7^\circ$, in a continuation of the local sheet of galaxies rather than the nearby voids.

A void population would be expected to have a range of properties, some with enough stars or gas to be detectable. SBS 0335-052 and DDO 154 are strange enough to motivate the thought that they are unusual members of this hypothetical void population, not extremes from known populations. But that does not agree with their positions, near galaxies.

These are just two examples. Systematic studies of environments of unusual galaxies, particularly early types, will be followed with interest.

3. STATISTICAL MEASURES

The tendency of less ordinary types of galaxies to avoid the voids defined by ordinary spirals has been probed by void probability functions (White 1979; Vogeley et al. 1994; El-Ad & Piran 2000; and references therein), two-point correlation functions, and nearest neighbor distances. To keep this discussion somewhat limited I discuss only the latter two, that have complementary features.

A particularly useful feature of correlation functions is the simple relation between the measurable angular function and the wanted spatial function. There is no simple relation between nearest neighbor distances in real space and the measurable nearest distances in projected angular distributions or in redshift space. But as discussed next, the interpretation of correlation functions as a probe of the void phenomenon is not straightforward. The rest of this paper accordingly uses nearest neighbor statistics.

3.1. Two-Point Statistics

One sees in Thompson’s (1983) maps the tendency of Markarian galaxies to avoid both dense regions and voids in the distribution of ordinary galaxies. The former means that on small scales the Markarian correlation function, ξ_{MM} , and the Markarian-optimally selected galaxy cross correlation function, ξ_{Mg} , are significantly less than the galaxy-galaxy function, ξ_{gg} . If at larger separations ξ_{MM} , ξ_{Mg} , and ξ_{gg} had similar values, because both galaxy types trace the same large-scale structure, the slopes of ξ_{MM} and ξ_{Mg} would be shallower than ξ_{gg} . This would not mean Markarian galaxies tend to occupy the voids defined by ordinary galaxies, of course. To the contrary, the visual impression from Thompson’s maps and the evidence from Thompson’s nearest neighbor statistic is that Markarian galaxies respect the voids.

The correlation functions for early- and late-type galaxies in Hermit et al. (1996 Figs. 10 and 11) behave as just described: at small separations later types have distinctly smaller correlation functions, while at separation $hr \sim 10$ Mpc the functions have similar values. This certainly demonstrates the small-scale morphology-density correlation. One sees from the example of Markarian galaxies that it need not imply later-type galaxies tend

to occupy the voids defined by earlier types.

If at $hr \gtrsim 10$ Mpc the correlation function for an unusual type of galaxy were unusually large it could be a signature of void galaxies. But because one can trace connections among occupied regions over quite large distances one would also have to consider the way the distributions of objects within occupied regions contribute to the abundances of galaxy pairs at large separations.

3.2. Nearest Neighbor Statistics

This measure also is affected by the morphology-density correlation, but it may reveal void galaxies through a tail in the distribution of nearest neighbor distances.

The test uses two types of objects. The *o*-type are reference ordinary galaxies, or the proposed equivalent in a simulation. The *t*-type are unusual test objects that may have tended to form in the unusual conditions in voids between concentrations of *o*-types. In analyses of observations the *t*-types may be galaxies — dwarf, irregular, compact, or low surface brightness — or gas clouds. In analyses of simulations the *t*-types would be mass concentrations that are not expected to develop into ordinary galaxies but seem to be capable of forming observable concentrations of stars or gas.

The distance from a *t*-type to the nearest *o*-type object is D_{to} , and the distance from an *o*-type to the nearest neighboring *o*-type is D_{oo} . The probability distribution of D_{to} depends on the number density of the reference *o*-type objects, but we have a control from the distribution of D_{oo} . If the two types were randomly selected from the same underlying population, and the two selection probabilities differed by a constant factor, the distributions of

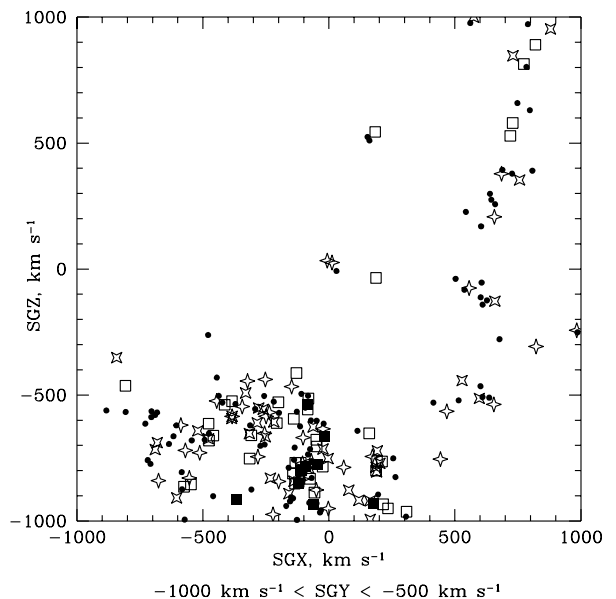


FIG. 2.— Map of Optical Redshift Survey galaxies in a slice in redshift space. The normal to the slice points in the direction of the Virgo Cluster, from the opposite side of the Milky Way. Filled squares are elliptical galaxies, open squares S0s, crosses Sa to Sb-c, plus signs later spiral types, and filled circles dwarfs and irregulars.

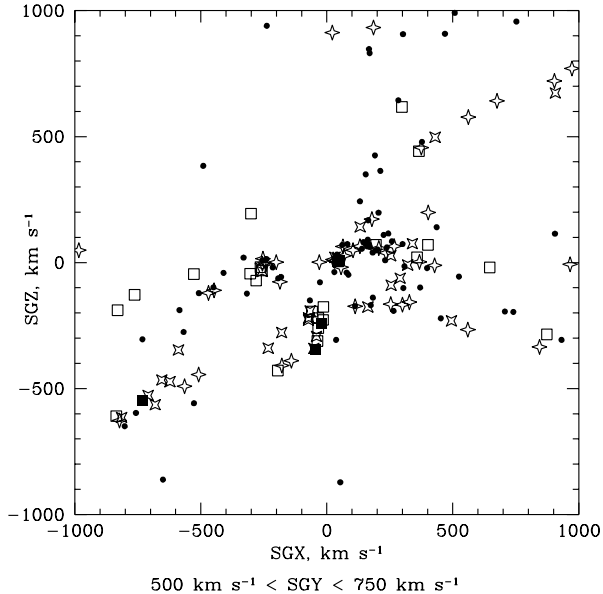


FIG. 3.— Map of ORS galaxies in a slice in redshift space on the same side of the Milky Way as the Virgo Cluster.

D_{to} and D_{oo} would be the same within the noise, even if the selection functions varied with position. If the t -types tended to be outside the concentrations of o -types it would produce a tail of large values in the distribution of D_{to} relative to D_{oo} .

All applications of this probe have used nearest neighbor distances in redshift space, which can be much larger than in real space (§3.3). The effect can be analyzed by using as separate variables the transverse and redshift separations, but this will be left for future work.

Early examples of this probe are in Soneira & Peebles (1977), who used it to test and argue against the idea that there is a spatially homogeneous population of field galaxies, and Thompson (1983), who introduced it to the analysis of voids.⁴

Nearest neighbor statistics have been applied to a considerable variety of candidate void objects (Eder et al. 1989; Salzer, Hanson, & Gavazzi 1990; Bothun et al. 1993; Pustil'nik et al. 1995; Linder et al. 1996; Lee et al. 2000). In some cases the nearest reference ordinary galaxy is about equally close to test and ordinary galaxies. In others the test sample have the more distant nearest neighbors. The difference is not very large, however. Thus one finds general agreement that all these classes of objects avoid the central parts of voids, but mixed opinions on consistency with the picture of biased galaxy formation. Two new applications of the statistic may help clarify the situation.

3.3. New Examples of the Nearest Neighbor Statistic

Redshift samples have improved, so an update of the nearest neighbor statistic is worthwhile. The example in §3.3.1 uses dwarfs plus irregulars as test galaxies, and in

⁴This study was used in §3.1 to illustrate the problematic interpretation of correlation functions as a measure of voids. But Thompson (1983) used nearest neighbor statistics, not correlation functions.

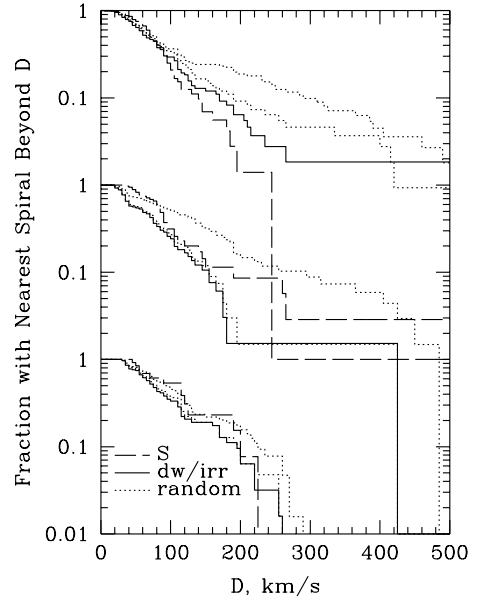


FIG. 4.— Distributions of distances D in redshift space of the nearest spiral neighbors of spirals (broken lines) and of dwarfs and irregulars (solid lines). The upper dotted lines show the effect of randomly shifting one in three of the dwarfs and irregulars, the lower dotted lines the effect of randomly shifting one in ten. The redshift ranges are $200 < cz < 500 \text{ km s}^{-1}$ in the bottom plot, $500 < cz < 750 \text{ km s}^{-1}$ in the middle, and $750 < cz < 1000 \text{ km s}^{-1}$ in the top.

§3.3.2 low surface brightness galaxies.

Both examples use the spirals in the Optical Redshift Survey (ORS; Santiago et al. 1995) as reference ordinary galaxies. At low redshift the ORS broadly samples the luminosity function, and it has useful information on morphology. The authors caution that completeness as a function of apparent magnitude and surface brightness varies across the sky; the selection may be particularly inhomogeneous for dwarfs and irregulars. The latter need not affect the relative distributions of D_{to} and D_{oo} if the ordinary galaxies are homogeneously sampled. And inhomogeneous sampling would not seem likely to mask the signature of void galaxies.

3.3.1. Redshift Maps

Figures 2 and 3 show maps of the ORS galaxies in nearby narrow slices in redshift space (corrected to the Local Group by adding to the heliocentric redshift 300 km s^{-1} toward $l = 90^\circ$ $b = 0$). The normals point to supergalactic coordinates $SGB = 0$, $SGL = 90^\circ$, roughly toward the Virgo Cluster. The slice in Figure 2 is on the opposite side of the Milky Way from the Virgo Cluster, the slice in Figure 3 on the same side. Galaxies closer than 6° from the Virgo Cluster are removed. The slice toward Virgo is thinner, because this side is more crowded, and it is seriously distorted by virgocentric flow, but early and late types may be similarly affected by large-scale streaming. Most parts of the slices are at high galactic latitude, but the upper right corner in Figure 2 and the lower left

TABLE 1
Nearest Neighbor Parameters

Test Sample	cz_{\min}^a	cz_{\max}^a	N_o	N_t	n_o^b	n_t^b	$H_o D_h^a$	$H_o \langle D_{oo} \rangle^a$	$\langle D_{to} \rangle / \langle D_{oo} \rangle$	$\langle D_{ro} \rangle / \langle D_{oo} \rangle$
Dw/Irr	200	500	20	63	0.08	0.26	11	110 ± 17	0.83 ± 0.14	1.43 ± 0.23
Dw/Irr	500	750	51	66	0.08	0.11	11	107 ± 16	0.69 ± 0.12	1.99 ± 0.32
Dw/Irr	750	1000	100	109	0.08	0.09	11	78 ± 5	1.10 ± 0.12	3.09 ± 0.26
LSBa	200	3000	153	27	0.02	0.003	38	133 ± 10	0.92 ± 0.14	2.51 ± 0.30
LSBb	200	3000	70	43	0.02	0.01	32	115 ± 10	0.88 ± 0.12	3.19 ± 0.36
LSBa	3000	6000	160	43	0.003	0.0008	180	284 ± 17	1.10 ± 0.12	1.68 ± 0.15
LSBb	3000	6000	80	60	0.004	0.003	140	270 ± 20	1.03 ± 0.10	1.81 ± 0.17
LSBa	6000	9000	106	42	0.0007	0.0003	560	490 ± 40	1.10 ± 0.12	1.39 ± 0.17

^aUnit km s⁻¹

^bUnit h³Mpc⁻³

corner of Figure 3 dip to $|b| < 30^\circ$, where the ORS may be significantly less complete.

The filled squares are elliptical galaxies (Burstein numerical morphological type $\text{BNMT} \leq 12$, de Vaucouleurs type $T \leq -5$; Willick et al. 1997, Table 7). The open squares are S0s (cut at $\text{BNMT} \leq 112$, $T \leq 0$), the crosses Sa through Sb-c (cut at $\text{BNMT} \leq 152$, $T \leq 4$), the plus signs later type spirals (cut at $\text{BNMT} \leq 182$, $T \leq 7$), and the filled circles all the dwarfs, irregulars, and other categories.

It is difficult to make out much difference in clustering properties of the different morphological types in Figures 2 and 3. It is easy to find nearly empty regions. The former is at least in part due to the absence of rich clusters. The latter may also be affected by the very limited samples, it agrees with the many other examples reviewed in §2 and §3.2.

3.3.2. Dwarfs and Irregulars

Results of the nearest neighbor test applied to the ORS Dw/Irr galaxies (filled circles in Figs. 2 and 3) and spiral galaxies (crosses and plus signs) are shown in Figure 4 and Table 1.

Pairs of ORS galaxies closer than 2 arc min and at low redshift tend to have the same or quite similar redshifts, a sign they may be the same galaxy, so one is discarded. I cut the galaxies at galactic latitude $|b| < 30^\circ$ and within 6° of the Virgo cluster ($\alpha = 186.6^\circ$, $\delta = 13.2^\circ$).

The subdivision in the three bins in redshift reduces the effect of variable completeness as a function of redshift, and it offers a test of reproducibility.

For each galaxy, o (spiral) or t (Dw/Irr), in each redshift bin, Figure 4 shows the distribution of distances in redshift space (relative to the Local Group) to the nearest o -type at any redshift greater than 200 km s^{-1} and within the cuts in angular position. The plots are normalized cumulative distributions.

In the two lowest redshift bins the Dw/Irr galaxies tend to have the closer spiral neighbor; in the highest redshift bin the spirals tend to have the closer spiral neighbor. The difference may be related to the variation in the range of absolute magnitudes sampled in each redshift bin (reflected in the variation in the ratio of numbers N_t and N_o of Dw/Irr and spirals). Or it may only be noise, for the differences in the distributions are small.

Table 1 shows the means $\langle D_{oo} \rangle$ of the distances of the nearest spiral neighbors of spirals, and the ratios $\langle D_{to} \rangle / \langle D_{oo} \rangle$ of the means of nearest neighbor distances of Dw/Irr and of spiral galaxies. The standard deviations assume each distance is statistically independent. (If two o -types are each other's nearest neighbor the distance counts once.) The differences of the distributions in Figure 4 may appear more significant than the differences of the ratios $\langle D_{to} \rangle / \langle D_{oo} \rangle$ from unity, because the cumulative distributions over-emphasize the noise.

We can estimate the nearest neighbor distance among spirals in real space from the observation that the small-scale distribution of optically selected galaxies approximates a scale-invariant clustering hierarchy, or fractal, with two-point correlation function $\xi = (r_o/r)^\gamma$. The distance r_h at which a spiral has on average one spiral neighbor satisfies

$$n_o \int_0^{r_h} \xi d^3r = \frac{4\pi n_o r_h^{3-\gamma} r_o^\gamma}{3-\gamma} = 1, \quad (1)$$

if the mean density n_o is large enough that $r_h \ll r_o$. Since the small-scale distribution is close to scale-invariant the mean D_h of the nearest neighbor distance differs from r_h by a fixed factor. Since the factor is not likely to be greatly different from unity a useful estimate of the mean real distance from a spiral to the nearest spiral is

$$D_h \sim \left(\frac{3-\gamma}{4\pi n_o r_o^\gamma} \right)^{1/(3-\gamma)}. \quad (2)$$

The table lists $H_o D_h$ for $hr_o = 5 \text{ Mpc}$ and $\gamma = 1.77$.

The small-scale relative peculiar velocity in the field is an order of magnitude larger than $H_o D_h$ in the ORS at $cz < 3000 \text{ km s}^{-1}$. This means the ratio $\langle D_{to} \rangle / \langle D_{oo} \rangle$ is determined by peculiar velocities; it does not tell us whether Dw/Irr or spiral galaxies tend to have the closer spiral neighbors in position space.

The D_{to} could be reduced by accidental cancellation of differences in the distributions of relative velocities and positions, but that seems unlikely. Thus I conclude

(1) the distributions of peculiar velocities of Dw/Irr and spiral galaxies relative to nearby spirals are quite similar, and

(2) the mean distance in position space from a Dw/Irr to the nearest spiral is less than about $1h^{-1} \text{ Mpc}$.

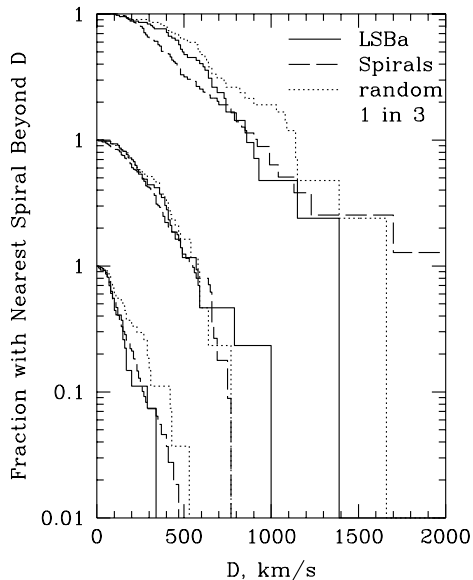


FIG. 5.— Distributions of distances of the nearest spiral neighbors of spirals and of Schombert et al. (1992) LSB galaxies. The dotted lines show the effect of randomly shifting one in three of the LSB galaxies. The redshift ranges are $200 < cz < 3000 \text{ km s}^{-1}$ in the bottom plot, $3000 < cz < 6000 \text{ km s}^{-1}$ in the middle, and $6000 < cz < 9000 \text{ km s}^{-1}$ in the top.

The second result depends on the number density of spirals, here $n_o \sim 0.1 h^3 \text{ Mpc}^{-3}$. But, since most spirals avoid the voids, if n_o were decreased by cutting the sample at larger luminosity or circular velocity, the Dw/Irr's would still tend to be within $1 h^{-1} \text{ kpc}$ of the concentrations of the sample spiral galaxies.

The last column in the table shows the result of moving each of the Dw/Irr galaxies to a randomly chosen position, with constant probability per unit solid angle within the cuts in galactic latitude and distance from the Virgo Cluster, and at uniformly probability distribution in z^3 within the redshift bin for the galaxy. The increase in nearest neighbor distances is significant, though not all that large.

The separate test illustrated by the upper dotted lines in Figure 4 shows the result of shifting to a random position one in three of the Dw/Irr (selecting every third object in the catalog list for a new position), leaving the rest at their catalog positions. The lower dotted lines show the effect of randomly repositioning one in ten. At one in three the resulting tail in the nearest neighbor distances is marginal in the shallowest sample, pronounced in the two deeper ones. It follows that at the catalog positions fewer than one in three of the Dw/Irr's could be members of a homogeneously distributed population, for otherwise the distributions of D_{to} for the other galaxies could not be tight enough to match the observed distribution of all D_{to} . When one in ten is randomly shifted the tail is pronounced only in the deepest sample. Thus I conclude

(3) fewer than about one in ten of the Dw/Irr is in a statistically homogeneous randomly distributed population.

3.3.3. Low Surface Brightness Galaxies

The Schombert et al. (1992; here LSBa) and Impey et al. (1996; here LSBb) low surface brightness galaxies are analyzed separately to check reproducibility. The reference ordinary galaxies are the ORS spirals used in §3.3.2.

Figure 5 shows the nearest neighbor distributions for the LSBa and ORS spiral galaxies at declination $10 < \delta < 25^\circ$, which includes most of the Schombert et al. (1992) low and very low surface brightness galaxies, at galactic latitude $|b| > 30^\circ$, and in the indicated ranges of redshift corrected to the Local Group. To be counted the nearest spiral neighbor must be more than 2 arc min away, to reduce the chance the same object is in both catalogs, and at $cz > 200 \text{ km s}^{-1}$, $0 < \delta < 35^\circ$, and $|b| > 30^\circ$. The cuts for LSBb (Fig. 6) are the same except for the declination: the galaxies whose neighbors are counted are at $-1.5^\circ < \delta < 3.5^\circ$, and the spiral neighbors are at $-11.5^\circ < \delta < 13.5^\circ$. The LSBb galaxies are the large angular size objects with HI redshifts in Impey et al. (1996). (The optical redshifts are not used because their uncertainties would significantly add to the nearest neighbor distances in redshift space.)

At the mean number density n_o of spirals in the nearest redshift bin, $200 < cz < 3000 \text{ km s}^{-1}$, the characteristic physical distance to the nearest neighbor in the clustering hierarchy is $H_o D_h \sim 35 \text{ km s}^{-1}$. As for the Dw/Irr case, this is small compared to typical relative peculiar velocities. The quite similar distributions of distances in redshift space to the nearest spiral neighbors of these LSBs, Dw/Irr's, and spiral galaxies, imply both LSB and Dw/Irr galaxies typically are closer than $1 h^{-1} \text{ Mpc}$ from a spiral and all three galaxy types have quite similar relative peculiar velocities.

In the deepest redshift bin (the bottom line in Table 1)

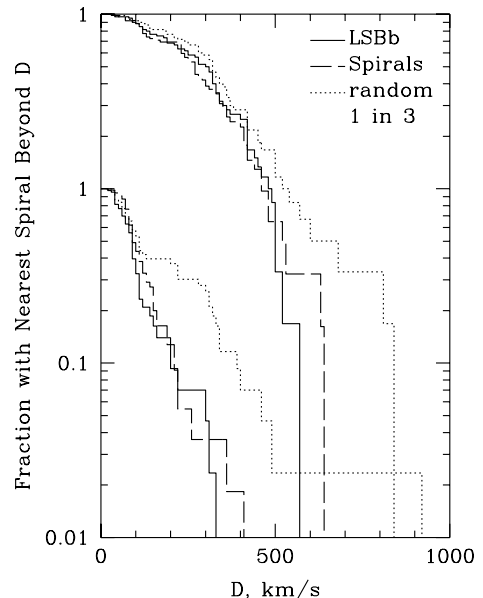


FIG. 6.— The same as Fig. 5 for the Impey et al. (1996) LSB galaxies at redshift ranges $200 < cz < 3000 \text{ km s}^{-1}$ in the bottom plot and $3000 < cz < 6000 \text{ km s}^{-1}$ in the top.

the mean nearest neighbor distance $\langle D_{ro} \rangle$ for randomly placed LSBa's is not significantly larger than the mean $\langle D_{to} \rangle$ at the catalog positions. This can be understood as follows. In a homogeneous random Poisson process with the mean number density $n_o = 0.0007h^3 \text{ Mpc}^{-3}$ of this sample of spirals the mean distance to the nearest neighbor is

$$D_{\text{Poisson}} = \frac{\Gamma(1/3)}{(36\pi n)^{1/3}} \sim 6h^{-1} \text{ Mpc}. \quad (3)$$

This is comparable to $\langle D_{oo} \rangle$ and to the clustering length r_o . This means the sparse sampling has suppressed the sensitivity of the nearest neighbor statistic to the galaxy distribution. Figure 6 for LSBb accordingly shows only the two lower redshift bins.

At the number density of spirals in the bin $3000 < cz < 6000 \text{ km s}^{-1}$ the physical distance $D_h \sim 150 \text{ km s}^{-1}$ in the clustering hierarchy is not much less than the relative velocity dispersion. The physical separations thus might be expected to make a significant contribution to the nearest neighbor distances in redshift space. Consistent with this, $\langle D_{oo} \rangle$ is not much larger than D_h .

The dotted lines in Figures 5 and 6 show the effect of randomly moving one in three of the LSB galaxies, leaving the rest at their catalog positions. The effect is marginal in some cases, but reproducible enough to show that fewer than one in three of the LSBs could be in a statistically homogeneously distributed population. Since most of this hypothetical homogeneous population would be in voids I conclude that

(4) the number density of observed LSB galaxies satisfies

$$n_{\text{LSB}} \lesssim 0.001h^3 \text{ Mpc}^{-3}. \quad (4)$$

Bothun et al. (1993) find that the nearest spiral neighbor of an LSB is on average 1.7 times further than that of a spiral galaxy. The difference from the results presented here is a cautionary example of the sensitivity to samples and methods of analysis.

Bearing in mind this example, but considering also the consistency of the distributions in Figures 5 and 6 from two independent low surface brightness samples and two redshift bins, I conclude that

(5) the mean nearest neighbor distances in redshift space for spirals and LSBs are not likely to differ by more than about 30 percent.

Since this analysis uses low surface brightness galaxies detected in HI the result is in line with the HI surveys in emission and absorption that show that gas clouds very distinctly prefer to be near galaxies (§2.3). But the quantitative constraints may be useful.

3.4. Summary of the Nearest Neighbor Measure

The candidate ordinary optically selected galaxies in a simulation of galaxy formation ought to define realistic voids. If the mean nearest neighbor distance among the candidate galaxies scales according to equation (2),

$$hD_h \sim 0.6 \left(\frac{0.01h^3}{n_o \text{ Mpc}^3} \right)^{0.8} \text{ Mpc}, \quad (5)$$

when the cut in luminosity function or circular velocity produces mean number density n_o , the distribution may

be expected to approximate the observed scale-invariant clustering hierarchy. In this case the voids likely are satisfactorily large.

Candidate void galaxies in a simulation of galaxy formation are the mass concentrations that are not good candidates for ordinary galaxies — perhaps their circular velocities are too small — but seem to be capable of developing into observable gas clouds or galaxies of stars. They might be candidates for Magellanic-type irregulars, with circular velocities greater than about $v_c \sim 20 \text{ km s}^{-1}$, large enough to resist substantial loss of photoionized plasma (Rees 1986; Babul & Rees 1992; Efstathiou 1992). Or they might be candidate low surface brightness or compact galaxies.

In the examples in §3.3 the mean physical distance from a Dw/Irr or LSB galaxy to the nearest spiral satisfies

$$\langle D_{to} \rangle_{\text{physical}} \lesssim 1h^{-1} \text{ Mpc}, \quad (6)$$

when the mean number density of spirals is

$$n_o \gtrsim 0.01h^3 \text{ Mpc}^{-3}. \quad (7)$$

The samples avoid rich clusters, that would increase the mean distances in redshift space and reduce them in real space. In redshift space equation (6) is replaced with an equality to about 10 percent.

At smaller n_o the examples in §3.3 indicate

$$\langle D_{to} \rangle_{\text{physical}} \lesssim 2\langle D_{oo} \rangle_{\text{physical}} \sim 2D_h. \quad (8)$$

The factor of two takes account of applications of the nearest neighbor test that find $\langle D_{to} \rangle > \langle D_{oo} \rangle$. In the examples presented here $\langle D_{to} \rangle$ and $\langle D_{oo} \rangle$ are equal to ~ 20 percent.

These numbers can be considered a quantitative definition of the void phenomenon. One must add the cosmic number density, n_t , because a model may satisfy equation (6) with a high density of void galaxies and an unacceptably high density of clustered objects. Equation (4) gives a limit on the density of candidate void LSB galaxies; the corresponding limit on void dwarf plus irregular galaxies is

$$n_{\text{Dw/Irr}} \lesssim 0.01h^3 \text{ Mpc}^{-3}. \quad (9)$$

More observational checks of these numbers would be of interest. The application to realizations of models for galaxy formation might interesting too.

4. THEORETICAL SITUATION

The conventional theoretical interpretation of voids was driven by the elegance of the Einstein-de Sitter model (with $\Omega_m = 1$ in matter capable of clustering, and negligibly small space curvature and cosmological constant), for this cosmological model requires most of the mass to be in the voids. It also is motivated by the CDM model for structure formation, which naturally produces a biased distribution of galaxies relative to mass. The considerations prior to the paradigm shift to $\Omega_m = 0.25 \pm 0.1$ are worth reviewing as a guide to the present situation.

4.1. Voids in an Einstein-de Sitter Universe

The small relative velocity dispersion in the CfA sample (Davis & Peebles 1983) shows that if $\Omega_m = 1$ then most of

the mass has to be in the voids.⁵ Davis et al. (1985; following Kaiser 1984 and Bardeen 1986) show this could occur in a natural way in the CDM model: if ordinary galaxies formed preferentially in high density regions they would be strongly clustered, leaving most of the mass in the voids. The void mass would be clumpy and thus might be expected to produce bound objects, some observable though different from ordinary galaxies. This seems intuitively reasonable (Peebles 1986, 1989). It is made quantitative in computations by Einasto et al. (1984), Dekel & Silk (1986), Brainerd & Villumsen (1992) and Hoffman, Silk & Wyse (1992).⁶

Opinions on whether the distributions of galaxy types argue for or against the CDM model are mixed. Arguments in favor cite morphological segregation (Dekel & Silk 1986), the smaller two-point correlation function for classes of unusual galaxies (Salzer, Hanson, & Gavazzi 1990; Mo, McGaugh & Bothun 1994), and low surface brightness galaxies (Hoffman, Silk & Wyse 1992). Section 3 presents reasons for treating these lines of evidence with some caution. Others conclude that the void phenomenon challenges biased galaxy formation (Einasto et al. 1984, Thuan, Gott & Schneider 1987; Eder et al. 1989; Peebles 1989; Binggeli, Tarengi & Sandage 1990; and Einasto et al. 1994).

Ostriker (1993) gives a balanced summary of the general opinion in the community shortly before the paradigm shift to low Ω_m : “Nominally one expects, in the CDM model, that the voids will be populated to a degree larger than is observed ... but in the absence of agreed-upon theories of galaxy formation, it is difficult to quantify this apparent disagreement.”

Ostriker’s assessment is accurate, but we do have guidance on what might have happened from what is observed (Peebles 1989). Consider the Magellanic-type irregulars on the outskirts of the Local Group — IC 1613, Sextans A and B, WLM, IC 5152, and NGC 3109 — at distances between 0.7 and 1.7 Mpc (Tully 1988; Table 1 in Peebles et al. 2000). They have small peculiar velocities relative to the Local Group. They are not near a large galaxy, so they are not likely to have been spawned by tidal tails or other nonlinear process in the large galaxies. Since they are at ambient densities close to the cosmic mean their first substantial star populations would have formed under conditions not greatly different from the voids at the same epoch. Why are such galaxies so rare in the voids?

4.2. Voids in a Low Density Universe

If $\Omega_m = 0.25 \pm 0.1$ the observations are consistent with the assumption that ordinary optically selected galaxies trace the mass (Bahcall et al. 2000 and references therein). If galaxies are good mass tracers we can assume the voids

⁵The relative velocity dispersion in the CfA sample is biased low by the under-representation of rich clusters with large velocity dispersions (Marzke et al. 1995). But the mass within the Abell radii of the Abell clusters is only about one percent of the critical Einstein-de Sitter value, and the low relative velocities of galaxies outside the clusters indicates the mass in the less dense galaxy concentrations sampled by CfA is significantly less than critical too.

⁶The cosmic string picture with hot dark matter (Scherrer et al. 1989), and the explosion variant (Ostriker, Thompson & Witten 1986), might produce voids that never were substantially disturbed, though that does not agree with the recent picture of a near space-filling Lyman- α forest at redshift $z \sim 3$.

contain little mass. This is the natural interpretation of the void phenomenon. But this consideration did not play a significant role in the change of the most favored model from Einstein-de Sitter to low Ω_m . I suspect one reason is the prediction by CDM simulations that the voids contain significant mass even when Ω_m is small.

A visual impression of numerical simulations of the low density Λ CDM model (with a cosmological constant to make flat space sections) is that of classical biasing: the larger dark mass halos cluster more strongly than the mass, and the less massive halos spread into the voids defined by the larger halos. It is no criticism of these studies, which report the behavior of the model, to note that one is not reminded of the void phenomenon illustrated in Figures 2 and 3. The situation is clearly presented in Figure 5 of Kauffmann et al. (1999).

The remedy may be a proper understanding of how the formation of observable objects may be suppressed in voids (Ostriker 1993). Rees (1985) explores the possible role of relativistic particles or ionizing radiation from the first generation of galaxies in suppressing subsequent galaxy formation, that otherwise would tend to occur in voids. Cen & Ostriker (2000) analyze realizations based on a numerical prescription for how galaxies form or are suppressed. They find the prescription produces observationally acceptable realizations. An application of the nearest neighbor statistic in §3.4 would be interesting. An explanation of the Im phenomenon (§4.1) would be edifying.

The remedy may be an adjustment of the CDM model. Bode, Ostriker & Turok (2000) show that warm dark matter can produce regions that are quite devoid of gravitational seeds for structure formation. The effect is striking, but the scale unfavorable. If in their Figure 11 the large circles represented ordinary optically selected galaxies, which would make about the observed number density, and the small circles were dwarfs or irregulars, the model would not seem to agree with the nearest neighbor distribution in Figure 4, or the maps in Figures 2 and 3. If the scale were enlarged so all circles represented ordinary $L \sim L_*$ galaxies, the voids would be well represented, but the Lyman- α forest at $z = 3$ would be a problem.

5. SUMMARY REMARKS

5.1. The Observational and Theoretical Situations

1. Some galaxy types prefer dense regions (Hubble 1936), others the edges of voids (Thompson 1983). This well-established morphology-density correlation (Dressler 1980) seems to arise in a natural way from hierarchical gravitational structure formation, as in the CDM model (White et al. 1987).

2. All known galaxy types and most gas clouds are scarce outside the concentrations of ordinary galaxies. This void phenomenon is discontinuous from the morphology-density correlation (§2). It appears to be a more challenging test of ideas on how galaxies formed (§4.2).

3. Two-point correlation functions are sensitive probes of the morphology-density correlation but, I argue in §3.1, are not readily interpreted measures of the void phenomenon.

4. The advantage of the nearest-neighbor statistic is a reasonably simple interpretation as a constraint on void

galaxies. This is widely recognized in the observational community (§3.2). The summary in §3.4 may be useful for testing simulations of galaxy formation.

5. The void phenomenon is observed among an impressively broad range of objects. The weight of this evidence naturally is from more readily observable gas-rich and star-forming objects, however. It may be significant that the considerations of Dekel & Silk (1986) argue for early-type void objects. Further observational tests for such objects are particularly desirable.

6. The challenge to the Λ CDM model might be resolved by a demonstration that the formation of observable void objects really can be adequately suppressed. This approach is challenged in turn by the Magellanic-type irregulars on the outskirts of the Local Group, that seem to have formed in ambient conditions not very different from the voids (§4.1).

7. The challenge might be resolved by adjusting the model for structure formation. A perhaps desperate idea is that the voids have been emptied by the gravitational growth of holes in the mass distribution (Peebles 1982). The void phenomenon seems striking enough to motivate a search for viable initial conditions for this picture.

5.2. Interpretations of Voids as an Example of the Scientific Method

The introduction of simulations of biased galaxy formation (Davis et al. 1985) was not inspired by or even obviously consistent with the evidence that giant and dwarf galaxies have quite similar distributions (Kirshner et al. 1981; Davis et al. 1982). This follows an honorable tradition in cosmology and, I suspect, other developing sciences. A strikingly successful example in cosmology is Einstein's (1918) cosmological principle. It did not agree with what was then known, but it led us to an aspect of physical reality.

The advances in ideas on structure formation since 1985 have not been seriously influenced by the void phenomenon. Again, this is not unusual. Another example is the galaxy n -point correlation functions. The near power law form of the observed two-point function is a widely discussed test. The three-point function is little noted in discussions of simulations, despite its importance in characterizing the small-scale galaxy distribution (Soneira & Peebles 1977). This complex and sometimes weak interplay of theory and practice in cosmology is well represented by Kuhn's (1962) paradigms, with socially selected theories and constraints. The weak interplay can be healthy. It allows a concentrated study of a particular subset of ideas, that may establish or eliminate them. It reduces the chance of distraction by misread evidence. It also allows distraction by unprofitable ideas, of course, but that is remedied when theory and practice mature and on occasion produce crises that drive paradigm shifts to better approximations to reality.

The CDM model is maturing, most dramatically in its success in relating the power spectrum of the thermal background radiation temperature to observationally acceptable cosmological parameters (eg. Hu et al. 2000). This shows the CDM model likely is a good approximation to how structure started forming on the length scales probed by the measurements.

The apparent inconsistency between the theory and ob-

servations of void is striking enough to be classified as a crisis for the CDM model. It may be resolved within the model, through a demonstration of an acceptable theory of galaxy formation. Or it may drive an adjustment of the model.

I have benefitted from discussions with Jerry Ostriker, Stacy McGaugh, Michael Strauss, Laird Thompson, Trinh Thuan, Brent Tully, and Neil Turok. This work was supported in part by the National Science Foundation.

REFERENCES

- Babul, A. & Rees, M. J. 1992, MNRAS, 255, 346
 Bahcall, N. A., Cen, R., Davé, R., Ostriker, J. P. & Yu, Q. 2000, astro-ph/0002310
 Bardeen, J. M. 1986, in Inner Space Outer Space, eds. E. W. Kolb, M. S. Turner, D. Lindley, K. Olive & D. Sekel (Chicago: the University of Chicago Press), p. 212
 Bergeron, J. & Boisse, P. 1991, AA, 243, 344
 Binggeli, B., Tarenghi, M. & Sandage, A. 1990, AA, 228, 42
 Bode, P., Ostriker, J. P. & Turok, N. 2000, astro-ph/0010389
 Bothun, G. D., Schombert, J. M., Impey, C. D., Sprayberry, D. & McGaugh, S. S. 1993, AJ, 106, 530
 Brainerd, T. G. & Villumsen, J. V. 1992, ApJ, 394, 409
 Carignan, C. C. & Freeman, K. C. 1988, ApJ, 332, L33
 Cen, R. & Ostriker, J. P. 2000, ApJ, 583, 83
 Chincarini, G. & Rood, H. J. 1976, ApJ, 206, 30
 Chincarini, G., Rood, H. J. & Thompson, L. A. 1981, ApJ, 249, L47
 Davis, M., Efstathiou, G., Frenk, C. S. & White, S. D. M. 1985, ApJ, 292, 371
 Davis, M., Huchra, J., Latham, D. W. & Tonry, J. 1982, ApJ, 253, 423
 Davis, M. & Peebles, P. J. E. 1983, ApJ, 267, 465
 Dekel, A. & Silk, J. 1986, ApJ, 303, 39
 de Lapparent, V., Geller, M. J. & Huchra, J. P. 1986, ApJ, 302, L1
 Dressler, A. 1980, ApJ, 236, 351
 Eder, J. A., Schombert, J. M., Dekel, A. & Oemler, A. 1989, ApJ, 340, 29
 Efstathiou, G. 1992, MNRAS, 256, 43P
 Einasto, J., Klypin, A. A., Saar, E. & Shandarin, S. F. 1984, MNRAS, 206, 529
 Einasto, J., Saar, E., Einasto, M., Freudling, W. & Gramann, M. 1994, ApJ, 429, 465
 Einstein, A. 1917, S.-B. Preuss. Akad. Wiss., 142
 El-Ad, H. & Piran, T. 2000, MNRAS, 313, 553
 Gregory, S. A. & Thompson, L. A. 1978, ApJ, 222, 784
 Grogin, N. A. & Geller, M. J. 2000, AJ, 119, 32
 Hermit, S., Santiago, B. X., Lahav, O., Strauss, M. A., Davis, M., Dressler, A. & Huchra, J. P. 1996, MNRAS, 283, 709
 Hoffman, G. L., Lu, N. Y. & Salpeter, E. E. 1992, AJ, 104, 2086
 Hoffman, Y., Silk, J. & Wyse, R. F. G. 1992, ApJ, 388, L13
 Hu, W., Fukugita, M., Zalduendo, M., & Tegmark, M. 2000, astro-ph/0006436
 Hubble, E. 1936, Realm of the Nebulae (New Haven: Yale University Press)
 Impey, C. D., Sprayberry, D., Irwin, M. J. & Bothun, G. D. 1996, ApJS, 105, 209
 Jõeveer, M., Einasto, J. & Tago, E. 1978, MNRAS, 185, 357
 Kaiser, N. 1984, ApJ, 284, L9
 Kauffmann, G., Colberg, J. M., Diaferio, A. & White, S. D. M. 1999, MNRAS, 303, 188
 Kirshner, R. P., Oemler, A., Schechter, P. L. & Shectman, S. A. 1981, ApJ, 248, L57
 Kuhn, B., Hopp, U. & Elsässer, H. 1997, AA, 318, 405
 Kuhn, T. S. 1962, The Structure of Scientific Revolutions (Chicago: University of Chicago Press)
 Lanzetta, K. M., Bowen, D. V., Tytler, D. & Webb, J. K. 1995, ApJ, 442, 538
 Lee, J. C., Salzer, J. J., Rosenberg, J. L. & Law, D. A. 2000, ApJ, 536, 606
 Lindner, U. et al. 1996, AA, 314, 1
 Marzke, R. O., Geller, M. J. da Costa, L. N. & Huchra, J. P. 1995, AJ, 110, 477
 Mayall, N. U. 1960, Annales d'Astrophysique, 23, 344
 Mo, H. J., McGaugh, S. S. & Bothun, G. D. 1994, MNRAS, 267, 129
 Ostriker, J. P. 1993, Ann. Rev. Astron. Ap., 31, 689
 Ostriker, J. P., Thompson, C. & Witten, E. 1986, Phys. Letters B, 180, 231

- Peebles, P. J. E. 1982, *ApJ*, 257, 438
Peebles, P. J. E. 1986, *Nature*, 321, 27
Peebles, P. J. E. 1989, *J. Roy. Astron. Soc. Canada* 1989, 83, 363
Peebles, P. J. E. 1993, *Principles of Physical Cosmology* (Princeton: Princeton University Press)
Peebles, P. J. E., Phelps, S. D., Shaya, E. J. & Tully, R. B. 2000, *astro-ph/0010480*
Popescu, C. C. Hopp, U. & Elsässer, H. 1997, *AA*, 325, 881
Postman, M. & Geller, M. J. 1984, *ApJ*, 281, 95
Pustil'nik, S. A., Ugryumov, A. V., Lipovetsky, V. A. Thuan, T. X. & Guseva, N. G. 1995, *ApJ*, 443, 499
Pustil'nik, S. A., Brinks, E., Thuan, T. X., Lipovetsky, V. A. & Izotov, Y. I. 2000, *astro-ph/0011291*
Rees, M. J. 1985, *MNRAS*, 213, 75P
Rees, M. J. 1986, *MNRAS*, 218, 25P
Rood, H. J. 1981, *Rept. Prog. Phys.*, 44, 1077
Salzer, J. J. 1989, *ApJ*, 347, 152
Salzer, J. J., Hanson, M. M. & Gavazzi, G. 1990, *ApJ*, 353, 39
Santiago, B. X., Strauss, M. A., Lahav, O., Davis, M., Dressler, A. & Huchra, J. P. 1995, *ApJ*, 446, 457
Scherrer, R. J., Melott, A. L. & Bertschinger, E. 1989, *PRL*, 62, 379
Schombert, J. M., Bothun, G. D., Schneider, S. E. & McGaugh, S. S. 1992, *AJ*, 103, 1107
Schombert, J. M., Pildis, R. A. & Eder, J. A. 1997, *ApJS*, 111, 233
Shull, J. M., Stocke, J. T. & Penton, S. 1996, *AJ*, 111, 72
Soneira, R. M. 1978, PhD dissertation, Princeton University
Soneira, R. M. & Peebles, P. J. E. 1977, *ApJ*, 211, 1
Soneira, R. M. & Peebles, P. J. E. 1978, *AJ*, 83, 845
Steidel, C. C., Dickinson, M., & Persson, S. E. 1994, *ApJ*, 427, L75
Szomoru, A., van Gorkom, J. H., Gregg, M. D. & Strauss, M. A. 1996, *AJ*, 111, 2150
Thompson, L. A. 1983, *ApJ*, 266, 446
Thuan, T. X., Gott, J. R. & Schneider, S. E. 1987, *ApJ*, 315, L93
Thuan, T. X. & Izotov, Y. I. 1997, *ApJ*, 489, 623
Tift, W. G. & Gregory, S. A. 1976, *ApJ*, 205, 696
Tully, R. B. 1988, *Nearby Galaxies Catalog* (Cambridge: Cambridge University Press)
Vanzi, L., Hunt, L. K., Thuan, T. X. & Izotov, Y. I. 2000, *astro-ph/0009218*
Vettolani, G., de Souza, R. E., Marano, B. & Chincarini, G. 1985, *AA*, 144, 506
Vogeley, M. S., Geller, M. J., Park, C. & Huchra, J. P. 1994, *AJ*, 108, 745
Weinberg, D. H., Szomoru, A., Guhathakurta, P. & van Gorkom, J. H. 1991, *ApJ*, 372, L13
White, S. D. M. 1979, *MNRAS*, 186, 145
White, S. D. M., Davis, M., Efstathiou, G. & Frenk, C. S. 1987, *Nature*, 330, 451
Willick, J. A., Courteau, S., Faber, S. M., Burstein, D., Dekel, A. & Strauss, M. A. 1997, *ApJ Suppl*, 109, 333
Zwaan, M. A., Briggs, F. H., Sprayberry, D. & Sorar, E. 1997, *ApJ*, 490, 173